Available online at www.sciencedirect.com
SCIENCE DIRECT
Biochemical Pharmacology 70 (2005) 229–241
Biochemical Pharmacology
www.elsevier.com/locate/biochempharm

Emodin induces apoptosis in human lung adenocarcinoma cells through a reactive oxygen species-dependent mitochondrial signaling pathway

Yu-Ting Su [a], Huei-Ling Chang [b], Song-Kun Shyue [c], Shih-Lan Hsu [d,e,f,*]

[a] *Institute of Medical Science, China Medical University, Taichung, Taiwan, ROC*
[b] *School of Medicine, China Medical University, Taichung, Taiwan, ROC*
[c] *Institute of Biomedical Sciences, Academia Sinica, Taipei, Taiwan, ROC*
[d] *Department of Education and Research, Taichung Veterans General Hospital No. 160, Section 3, Chung-Gang Road, Taichung, Taiwan, ROC*
[e] *Institute of Toxicology, Chung Shan Medical University, Taichung, Taiwan, ROC*
[f] *Institute of Chinese Pharmaceutical Sciences, China Medical University, Taichung, Taiwan, ROC*

Received 18 January 2005; accepted 8 April 2005

Abstract

Emodin, a natural anthraquinone derivative isolated from *Rheum palmatum* L., has been reported to exhibit anti-cancer effect on several human cancers such as liver cancers and lung cancers. However, the molecular mechanisms of emodin-mediated tumor regression have not been fully defined. In this study, we show that treatment with 50 μM emodin resulted in a pronounced release of cytochrome *c*, activation of caspase-2, -3, and -9, and apoptosis in human lung adenocarcinoma A549 cells. These events were accompanied by the inactivation of ERK and AKT, generation of reactive oxygen species (ROS), disruption of mitochondrial membrane potential ($\Delta\psi_m$), decrease of mitochondrial Bcl-2, and increase of mitochondrial Bax content. Ectopic expression of Bcl-2, or treatment with aurintricarboxylic acid, furosemide or caspase inhibitors markedly blocked emodin-induced apoptosis. Conversely, pharmacologic ERK and AKT inhibition promoted emodin-induced apoptosis. Furthermore, the free radical scavenger ascorbic acid and *N*-acetylcysteine attenuated emodin-mediated ROS production, ERK and AKT inactivation, mitochondrial dysfunction, Bcl-2/Bax modulation, and apoptosis. Take together, these findings suggest that in A549 cells, emodin-mediated oxidative injury acts as an early and upstream change in the cell death cascade to antagonize cytoprotective ERK and AKT signaling, triggers mitochondrial dysfunction, Bcl-2 and Bax modulation, mitochondrial cytochrome *c* release, caspase activation, and consequent leading to apoptosis.

Keywords: Emodin; ROS; Bcl-2 family; Cytochrome *c*; Caspase; Apoptosis

1. Introduction

Lung cancer is the leading cause of male and female cancer death worldwide. Every year, about 7000 people die of lung carcinoma, and the number is increasing rapidly in Taiwan. Lung cancers are classified into small cell lung cancer (SCLC) and non-small cell lung cancer (NSCLC, including adenocarcinoma, squamous cell carcinoma, and large cell carcinoma). NSCLC is the more common variant (~80% of lung cancers) and, unlike SCLC, is less sensitive

Abbreviations: Adv, adenovirus; ATA, aurintricarboxylic acid; DAPI, 4′,6-diamindino-2-phenylindole; DCF-DA, 2′,7′-dichlorofluorescensin diacetate; DEVD-AFC, Asp-Glu-Val-Asp-7-amino-4-trifluoromethyl coumarin; $DiOC_6$, 3,3-dihexyloxacarbocyanine iodide; Emodin, 1,3,8-trihydroxy-6-methyl anthraquinone; ERK, extracellular signal-regulated protein kinase; HE, dihydroethidine; IETD-AFC, Ile-Glu-Thr-Asp-7-amino-4-trifluoromethyl coumarin; LEHD-AFC, Leu-Glu-His-Asp-7-amino-4-trifluoromethyl coumarin; MAPkinase, mitogen-activated protein kinase; NAC, *N*-acetyl-cysteine; PI_3 kinase, phosphatidylinositol 3′-kinase; TUNEL, terminal transferase-mediated dUTP-fluorecensin nick end-labeling; U0126, 1,4-Diamino-2,3-dicyano-1,4-bis (2-aminophenylthio) butadiene; YVAD-AFC, Tyr-Val-Ala-Asp-7-amino-4-trifluoromethyl coumarin; VDVAD-AFC, Val-Asp-Val-Ala-Asp-7-amino-4-trifluoromethyl coumarin; VEID-AFC, Val-Glu-Ile-Asp-7-amino-4-trifluoromethyl coumarin; z-VDVAD-fmk, z-Val-Asp-Val-Ala-Asp-fluoromethyl ketone; z-DEVD-fmk, z-Asp-Glu-Val-Asp-fluoromethyl ketone; z-IETD-fmk, z-Ile-Glu-Thr-Asp-fluoromethyl ketone; z-LEHD-fmk, z-Leu-Glu-His-Asp-fluoromethyl ketone

* Corresponding author. Tel.: +886 4 23592525x4037; fax: +886 4 23592705.
E-mail address: h2326@vghtc.vghtc.gov.tw (S.-L. Hsu).

0006-2952/$ – see front matter © 2005 Elsevier Inc. All rights reserved.
doi:10.1016/j.bcp.2005.04.026

to chemotherapeutic agents. Survival statistics are dismal with an average 5-year survival of 10–15% [1]. Thus, it is crucially important to develop better therapeutic strategies for the management of NSCLC. It is well known both growth inhibition and apoptosis are the important determinants of the response of cancers to chemotherapeutic agent [2–4]. Therefore, compounds that induce cell-cycle arrest and apoptosis may provide potent anti-cancer effect for cancer treatment.

Natural herbal medicines such as *Rheum palmatum* L. (Polygonaceae) is traditionally applied in cancer therapy in Chinese medicine. Emodin (1,3,8-trihydroxy-6-methylanthraquinone) is an active constituent isolated from the root of *R. palmatum* L. [5]. Pharmacological studies have demonstrated that emodin possesses anti-bacterial [6], anti-inflammatory [7], immunosuppressive [8], vasorelaxant [9], anti-ulcerogenic [10], and anti-cancer effects. Previous studies have demonstrated that emodin inhibits cell growth in several type of tumor cells [3,11–16]. Relevant to its anti-proliferative activity, emodin is a potent inhibitor of the protein tyrosine kinase [17], was shown to suppress HER-2/neu tyrosine kinase activity in HER-2/neu-overexpressing human breast and lung cancer cells in vitro and inhibition of malignant transformation and metastasis-associated properties of HER-2/neu-overexpression breast cancer cells in vivo. It has also been reported that emodin can enhance the sensitivity of cancer cells to chemotherapeutic agents [13,18,19]. However, the molecular mechanism of emodin-mediated chemotherapeutic effect on cancer cells remains unclear. The clarification of the mode of action of emodin may be important in developing its application. In this study, we found that emodin-induced apoptosis was via a ROS- and Bcl-2/Bax-dependent mitochondrial signaling pathway in human lung adenocarcinoma A549 cells.

2. Materials and methods

2.1. Reagents

Emodin (1,3,8-trihydroxy-6-methylanthraquinone), furosemide (Furo), and aurintricarboxylic acid (ATA), 4′,6-diamindino-2-phenylindole (DAPI), ascorbic acid (Asc), and *N*-acetylcysteine (NAC) were purchased from Sigma, St. Louis, MO. Anti-Bcl-2, anti-Bcl-X_{L-S}, anti-Bad, anti-phospho-ERK, anti-AKT, and anti-Bax, were purchased from Santa Cruz Biotechnology (Santa Cruz, CA); anti-Bak, anti-Bid, anti-caspase-8, and anti-cytochrome *c* were purchased from PharMingen (San Diego, CA). Anti-phospho-AKT and U0126 (1,4-diamino-2,3-dicyano-1,4-bis(2-aminophenylthio) butadiene) were purchased from Cell Signaling Technology, Inc. (Beverly, MA, USA). Anti-β-Actin was purchased from Oncogene Science, Inc. (Uniondale, NY). Anti-ERK was purchased from Calbiochem Chemical Company (CN Biosciences Notts, UK). Anti-cytochrome oxidase IV was obtained from Molecular Probes (Eugene, OR, USA). Anti-mouse and anti-rabbit IgG peroxidase-conjugated secondary antibody were purchased from Amersham (Buckinghamshire, UK). The recombination Bcl-2-adenoviral vector and control adenoviral vector were provided by Dr. Song-Kun Shyue at the Institute of Biomedical Sciences, Academia Sinica (Taipei, Taiwan). TUNEL assay kit was obtained from Roche Diagnostics (Mannheim, Germany). Caspase-2 inhibitor (z-VDVAD-fmk), caspase-3 inhibitor (z-DEVD-fmk), caspase-8 inhibitor (z-IETD-fmk), and caspase-9 inhibitor (z-LEHD-fmk) were purchased from KAMIYA. Caspase activity assay kits, including the fluorogenic substrates of caspase-1 (YVAD-AFC), caspase-2 (VDVAD-AFC), caspase-3 (DEVD-AFC), caspase-6 (VEID-AFC), caspase-8 (IETD-AFC) and caspase-9 (LEHD-AFC), were purchased from R&D systems (Minneapolis, MN, USA). 2′,7′-Dichlorofluorescensin diacetate (DCF-DA), dihydroethidine (HE), and 3,3-dihexyloxacarbocyanine iodide ($DiOC_6$) were purchased from Molecular Probes (Eugene, OR, USA).

2.2. Cell culture and cytotoxicity assay

Human lung adenocarcinoma cell line A549, human non-small cell cancer line H460, human squamous carcinoma cell line CH27, human fibroblast-like lung cell line (WI-38), endothelial cells (prepared from 4-day-old neonatal Sprague–Dawley rat hearts as described elsewhere) [20], hepatic stelle cells and hepatocytes (prepared from adult Sprague–Dawley rat liver as described elsewhere) [21] were cultured in Dulbecco's modified Eagle's medium (Flow Laboratories), containing 10% fetal calf serum, antibiotics 100 U/ml penicillin and 100 μg/ml stretomycin, and 2 mM glutamine, at 37 °C in a humidified atmosphere comprising 95% air and 5% CO_2. Culture medium was changed every 2 days. For growth inhibition assay, cells were seeded into 12-well plates at a density of 1×10^5 cells/well. After 24 h, cells were treated with various concentrations of emodin for the indicated time points. After treatment, the number of viable cells was determined by Trypan blue dye exclusion method.

2.3. Clonogenic assay

Clonogenic assay was performed by seeding 250 cells per well into 6-well plastic dishes. After 24-h incubation, cells were treated with various concentrations (0, 1, 5, 10, and 25 μM) of emodin for 72 h. After treatment, cells were washed twice with PBS to remove any remaining emodin and fresh medium was added. The cells were incubated for another 14 days. The colonies were stained using crystal violet [22]. Colonies of greater than 50 cells were counted as surviving, and the percent survival was determined using

the following equation: percentage of survival = (colonies of drug treatment/colonies of control) × 100.

2.4. Apoptotic cell determination

A549 cells were treated with 50 μM emodin for 48 h, then washed with phosphate-buffered saline (PBS) twice, fixed in 2% paraformaldehyde for 30 min and then permeabilized with 0.1% Triton X-100/PBS for 30 min at room temperature. After washing with PBS, terminal transferase-mediated dUTP-fluorescensin nick end-labeling (TUNEL) assay was performed according to the manufacturer's instructions (Boehringer Mannheim). Cells were incubated in TUNEL reaction buffer in a 37 °C humidified chamber for 1 h in the dark, then rinsed twice with PBS and incubated with DAPI (1 μg/ml) at 37 °C for 10 min, stained cells were visualized using a fluorescence microscope. Fluorescence intensity changes were detected under a fluorescence microscope or analyzed by flow cytometry. TUNEL-positive cells were counted as apoptotic cells.

2.5. Caspase activity assay

Cells lysates obtained from emodin-treated or untreated A549 cells were tested for caspase-2, -3, -6, -8, and -9 activities by addition of a caspase-specific peptide substrate conjugated with the fluorescent reporter molecule 7-amino-4-trifluoromethyl coumarin (R&D System Minneapolis, USA). The cleavage of the peptide by the caspase releases the fluorochrome that when excited by light at 400 nm emits fluorescence at 505 nm. The level of caspase enzymatic activity in the cell lysate is directly proportional to the fluorescence signal detected with a fluorescent microplate reader (Fluoroskan Ascent; Labsystems, Finland).

2.6. Preparation of subcellular fractions

Cell fractionation was performed as described previously with some modifications [23,24]. Briefly, cells were collected at different time intervals and washed twice in ice-cold PBS. Cell pellets were frozen at −80 °C, thawed at 4 °C, and resuspended in cytosol extraction buffer (50 mM Tris, pH 7.4, 4 mM EDTA, 2 mM EGTA, 1 mM sodium orthovanadate, 1 mM sodium fluoride, 5 μg/ml leupeptin, 5 μg/ml aprotinin, 0.2 mM phenylmethylsulfonylfluoride, 0.5 mM DTT) at 4 °C until more than 95% of the cells were Trypan blue positive. Cell lysates was centrifugated at 100,000 × *g* for 30 min at 4 °C, the supernatant was collected as the cytosolic fraction. The pellet was resuspended in modified RIPA buffer (50 mM Tris, pH 7.4, 150 mM NaCl, 1 mM EGTA, 5 mM EDTA, 0.5% Triton X-100, 0.25% sodium deoxycholate, 1 mM sodium fluoride, 1 mM sodium orthovanadate, 5 μg/ml leupeptin, 0.2 mM phenylmethyl-sulfonylfluorid, aprotinin, and 10 mg/ml, 0.5 mM DTT) at 4 °C overnight and centrifuged. The supernatant was collected as the particulate fraction. Protein concentrations were determined using the Bradford method and samples were frozen as aliquoted at −80 °C for subsequent experiments. The particulate fraction includes membrane-organelle proteins and nuclear-associated proteins.

2.7. Protein preparation and immunoblotting

Cells were cultured without or with 50 μM emodin at various times. After treatment, both adherent and floating cells were harvested, washed twice with ice-cold PBS and lysed in ice-cold modified RIPA buffer. After 30 min of incubation on ice, cells were centrifuged at 100,000 × *g* for 30 min at 4 °C, supernatants were collected. Protein concentration was determined using the Bradford method. For Western blot analysis, equal amounts of total protein were loaded onto SDS-polyacrylamide gels and the proteins electrophoretically transferred onto a PVDF membrane (Millipore, Bedford, MA). Immunoblots were analyzed using specific primary antibodies. After exposure to horseradish peroxidase-conjugated secondary antibody for 1 h, proteins were visualized using an enhanced chemiluminescence detection kit (ECL Kits; Amersham Life Science).

2.8. Measurement of intracellular ROS generation and mitochondrial membrane potential ($\Delta\psi_m$)

It is well documented that HE is a specific superoxide tracing dye, and DCF-DA has been used frequently to monitor H_2O_2 and hydroxyl radical levels in cells. The cells were incubated with 50 μM emodin for the indicated periods. For determination of mitochondrial membrane potential, cells were treated with 10 μM HE, 5 μM DCF-DA 30 min prior to harvesting, then washed with PBS. The fluorescence intensity of the cells was determined by flow cytometry.

Changes of mitochondrial membrane potential ($\Delta\psi_m$) have been considered to be an indicator of mitochondrial damage. Cells were treated with 50 μM emodin for the indicated periods. Cells were incubated with $DiOC_6$ (40 nM in culture medium) 30 min prior to harvesting, then washed with PBS, cellular uptake of $DiOC_6$ was analyzed by flow cytometry.

2.9. Statistical analysis

All data are presented as mean ± S.D. of at least nine replicates from three separate experiments. Statistical differences were evaluated using the Student's *t*-test and considered significant at the $^{*}P < 0.05$, $^{**}P < 0.01$, or $^{***}P < 0.001$ level. All the figures shown in this article were obtained from at least three independent experiments with similar results.

3. Results

3.1. Emodin caused growth inhibition and apoptotic cell death

The effect of emodin on cell growth and cell death were examined in three human lung cancer cell lines. As shown in Fig. 1A, treatment of lung cancer cells with low concentration of emodin (10 μM) resulted in growth inhibition but not cell death, approximately 40, 60, and 90% growth inhibition was detected after 72 h treatment of A549, H460, and CH27 cells, respectively. However, emodin-mediated cytotoxicity occurred at a concentration greater than 25 μM. Clonogenic assays were used to confirm the cytotoxic effect of various concentrations of emodin on three tested cell lines. As shown in Fig. 1B, the clonogenic survival of A549, H460, and CH27 cells were not significantly affected by exposure to emodin for 48 h, compared to that of the controls, at the concentrations between 1 and 10 μM. However, treatment with 25 μM emodin markedly reduced long-term colony formation to 35 ± 7% (A549 cells), 37 ± 6% (H460 cells), and 48 ± 6% (CH27 cells), as compared to untreated controls (100%). These data indicated that low concentrations (1–10 μM) of emodin treatments resulted in a cytostatic effect, but not cytotoxic effect, in all three tested cell lines. Investigations of high concentration (>25 μM) emodin-treated cells under an inverted phase microscope revealed that cells exhibited morphological features of apoptosis. To obtain further support for the induction of apoptosis by emodin in

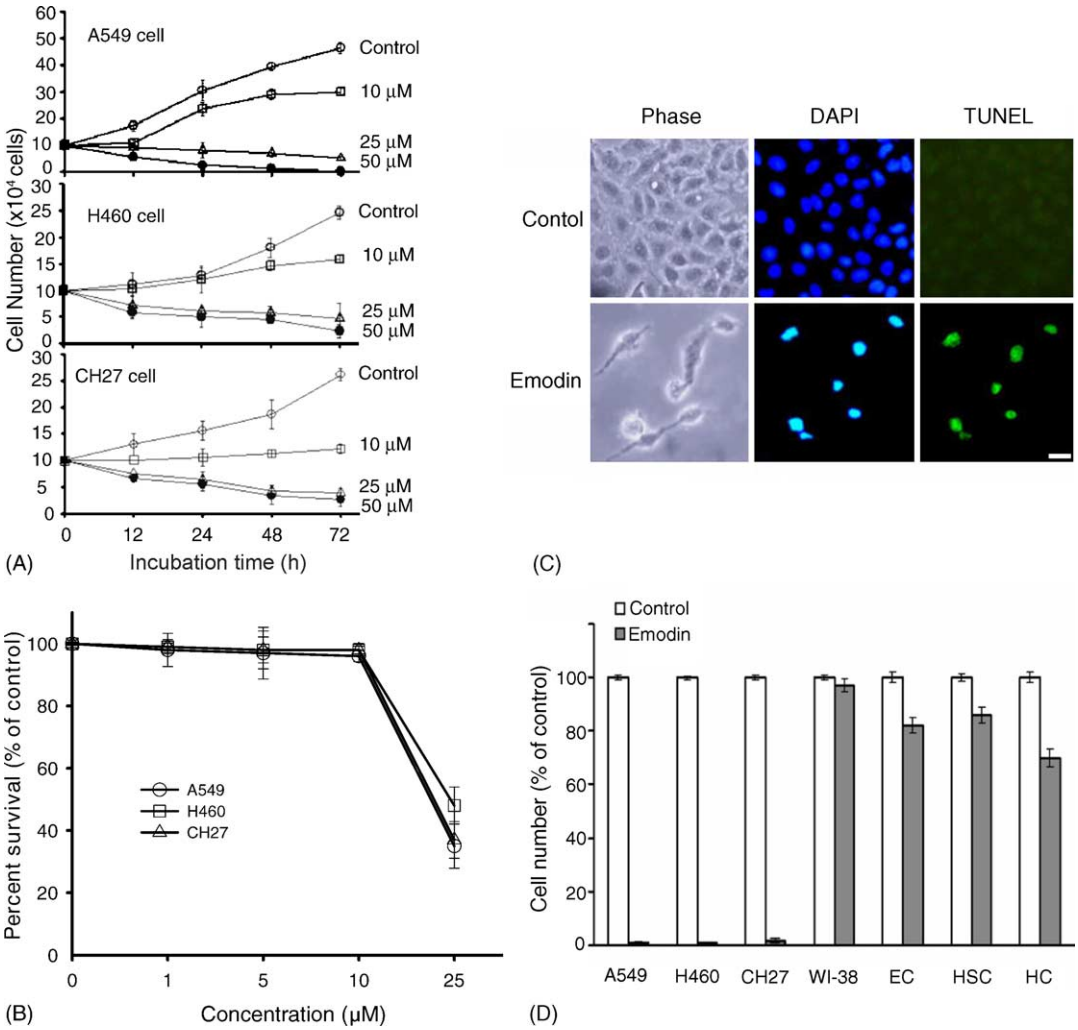

Fig. 1. Induction of apoptosis by emodin. (A) A549, CH27, and H460 cells were treated without or with 10, 25, and 50 μM of emodin, for 12, 24, 48, and 72 h. Cell numbers were calculated by Trypan blue dye exclusion method using hemocytometer. Data are presented as mean ± S.D. of nine replicates from three independent experiments. (B) Effect of emodin on colony formation. A549, H460, and CH27 cells were treated with various concentrations (0, 1, 5, 10, and 25 μM) of emodin for 72 h. After treatment, cells were washed and cultured in drug-free medium for another 14 days. Stained colonies were counted. (C) A549 cells were treated with 50 μM emodin for 48 h, nuclei were characterized by DAPI and TUNEL assay and investigated under a fluorescent microscopy. Magnification 200×; scale bar, 20 μm. (D) The effect of emodin on several types of cells. A549, CH27, H460, WI-38, rat endothelial cells (EC), rat hepatic stellate cells (HSC) and rat hepatocytes (HC) were treated without or with 50 μM emodin for 96 h. Cell number was measured by trypan blue dye exclusion method.

A549 cells, DAPI staining and in situ TUNEL assay were performed. As demonstrated in Fig. 1C, treatment with 50 μM emodin for 48 h significantly induced the apoptotic cell death with condensed nuclei and increase of TUNEL positive cells, suggesting that the DNA fragmentation was occurring in these cells. Next, the cytotoxic effects of emodin were examined in human fibroblast-like lung WI-38 cells and three primary cultured rat normal cells, including neonatal rat heart endothelial cells, rat hepatocytes, and rat hepatic stellate cells. Results showed that emodin (50 μM) evoked a significant growth inhibitory effect, but a less or no cytotoxic effect in four tested normal cells after 96 h treatment (Fig. 1D). These data indicate that normal cells were more resistance to emodin-mediated cytotoxicity than lung cancer cells.

3.2. Emodin-induced apoptosis via caspase activation

Caspases are a family of cysteine proteases that plays a central role during the executional phase of apoptosis [25]. To explore whether emodin induces apoptosis by activation of caspases, fluorogenic peptide substrates were used to detect specific caspase activity. The results shown in Fig. 2A, caspase-9, -2, and -3 were activated in A549 cells after 12 h emodin treatment. The marked activation of caspase-2, -3, and -9 was observed after 24 h emodin treatment. However, the caspase-8 and -6 were slightly activated during late stage of emodin-induced apoptosis. To further confirm the activation of caspase-2, -3, -8, and -9, specific antibodies were used to detect the proteolytically activated fragments of each caspase (Fig. 2B). Results showed that the active fragments of caspase-2,-3, and -9 were observed at 12 h after emodin treatment while cleaved caspase-8 fragment was detected after 24 h emodin treatment. To explore whether the activation of caspases was required for induction of apoptosis by emodin. A549 cells were co-treated with caspase inhibitors and emodin. As depicted in Fig. 2C, incubation with the inhibitor of caspase-9 (z-LEHD-fmk), caspase-2 (z-VDVAD-fmk), or caspase-3 (z-DEVD-fmk) significantly blocked emodin-triggered apoptosis in A549 cells. Whereas, the caspase-8 inhibitor (z-IETD-FMK) was less effective to inhibit emodin-triggered apoptosis. These observations indicated that activation of caspase cascade might play a crucial role in emodin-induced apoptotic death in A549 cells.

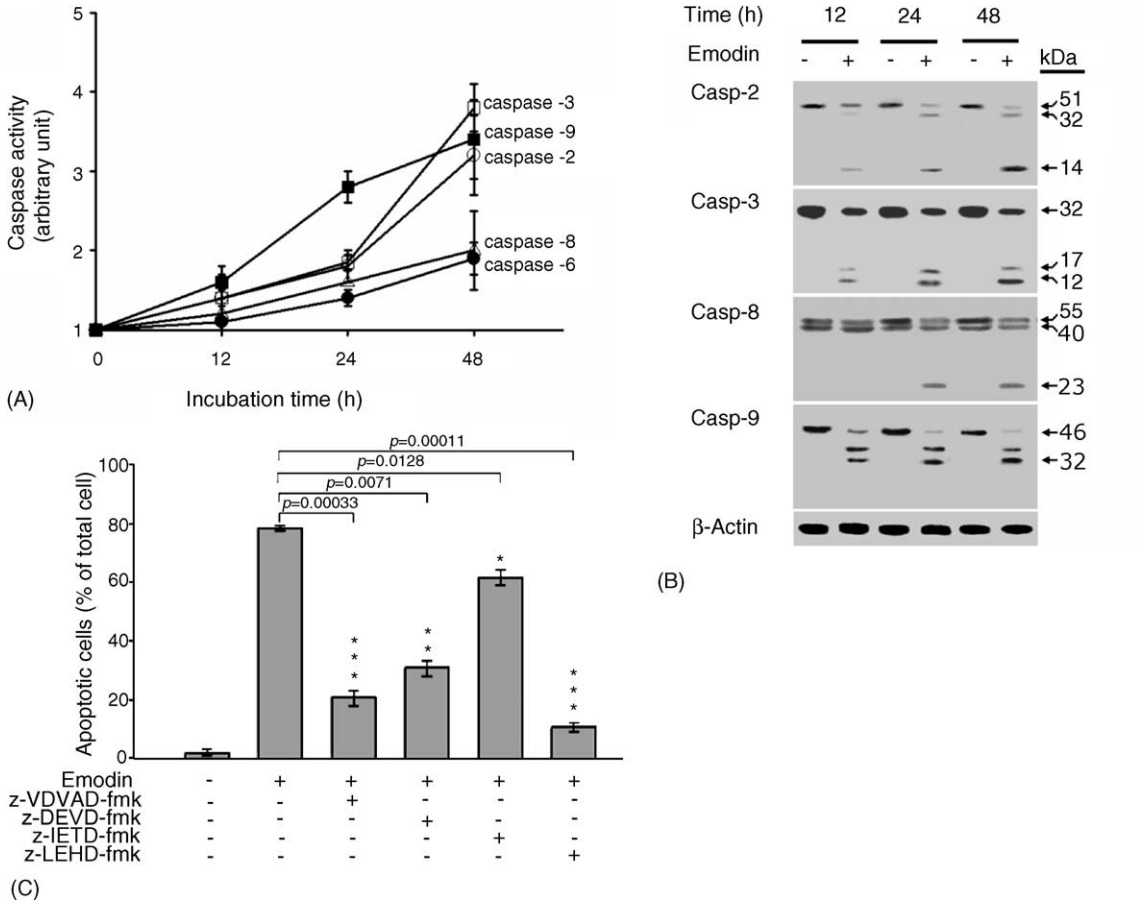

Fig. 2. Involvement of caspase activation in emodin-induced apoptosis. A549 cells were treated with 50 μM emodin for the indicated time periods. Extracts from untreated or emodin-treated cells were assayed for (A) caspase activity using fluorogenic peptide substrate or (B) by Western blot analysis. (C) Caspase inhibitors inhibited emodin-induced apoptosis. A549 cells were treated with 50 μM emodin in the presence or absence of caspase inhibitors (100 μM). After 48 h incubation, apoptotic cells were calculated by TUNEL assay.

3.3. Generation of ROS, disruption of mitochondrial membrane potential ($\Delta\psi_m$) and release of mitochondrial cytochrome c

It is generally assumed that after the loss of the outer mitochondrial membrane integrity and the release of cytochrome *c* from the mitochondria to the cytosol, the cells are committed to apoptosis [26]. It has also been reported that production of reactive oxygen species (ROS) contribute to mitochondrial damage that may facilitate the further release of ROS into the cytoplasm [27]. To address the possibility that the emodin-induced apoptosis could be related to contributions from the mitochondrial pathway, A549 cells were treated with 50 μM emodin for the indicated time periods, the change in ROS production and $\Delta\psi_m$ were examined using the specific fluorescence probes, DCF-DA, dihydroethidine and $DiOC_6$ [3]. As indicated in Fig. 3A, exposure to emodin induced a left shift of the $DiOC_6$ fluorescence curves. This is indicative that the emodin treatment induced an disruption of $\Delta\psi_m$. In contrast, administration of emodin resulted in a right shift of the DCF-DA and dihydroethidine fluorescence curves, indicating the increase in ROS generation. The relative levels of ROS were elevated as early as 0.5 h after emodin treatment and persistently increased with exposure time. The levels of $\Delta\psi_m$ and ROS in untreated control cells were unchanged over all of the incubation time periods. Next, the effect of emodin on the cytochrome *c* release from mitochondria into the cytosol was examined. After administration of A549 cells to 50 μM emodin, a gradual increase of cytosolic cytochrome *c* starting at 1 h, a reduction at 6 h, whereas at 48 h, there was a 8-fold increase in their levels in the cytosol (Fig. 3B), suggesting the cytochrome *c* release was biphasic.

3.4. Involvement of Bcl-2 family proteins in emodin-induced apoptosis

Because the disruption of $\Delta\psi_m$ was not correlated with the peak release of cytochrome *c* into the cytosol after exposure of A549 cells to emodin, we examined other possible mechanism for the cytochrome *c* release into the cytosol at later time points. Previous report indicated that the Bcl-2 family molecules regulate the release of cytochrome *c* from the mitochindria [28]. The levels of Bcl-2 family members were detected by Western blot analysis. As shown in Fig. 4A, exposure of A549 cells with 50 μM emodin caused in a significant decrease in Bcl-2 while increase in Bax protein levels after 24 h treatment. However, the expression levels of Bak, Bcl-X_L, Bcl-X_S, Bid, and Bad proteins were not affected by emodin. Bcl-2 has been shown to localize to mitochondrial membrane and stabilize mitochondrial functions, thereby suppressing the release of pro-apoptotic effector molecules. Conversely, Bax translocation to the mitochondria induces cytochrome *c* release from mitochindria [29]. Next, cell fractionation study was done, the levels of Bcl-2 and Bax in the cytosol and particulate were monitored by Western blotting after treatment with emodin. As depicted in Fig. 4B, a significant increase in the levels of Bax and decrease of Bcl-2 in the mitochondrial membrane at later time points of emodin treatment (24 and 48 h). To define the role of Bcl-2 and Bax in emodin-induced apoptosis, A549 cells were transduced with 50 moi (multiplicity of infection) of adeno-Bcl-2 and control adenoviral vectors. As shown in Fig. 4C, infection with adeno-Bcl-2 viral vector increased the intracellular Bcl-2 levels by 2.5-fold. Overexpression of Bcl-2 protein in A549 cell significantly protected against emodin-induced apoptotic death. In addition, treatment of A549 cells with furosemide (an inhibitor of Bax translocation) [30] resulted in a markedly attenuated the emodin-induced apoptosis in a dose-dependent manner (Fig. 4D).

3.5. Inactivation of AKT or ERK affected the sensitivity of emodin-induced apoptosis

It has been shown that AKT modulates cell survival and apoptosis at a premitochondiral stage by preventing Bax conformation change and its translocation to the mitochondria [31]. To address the effect of emodin on AKT, cells were treated with emodin for various time periods, Western blot analysis was done to detect the levels of phosphorylated AKT. As shown in Fig. 5A, exposure of A549 cells to emodin caused in a marked decrease in phosphorylated AKT (Thr 308 and Ser 473) after 24 and 48 h treatment. Growing evidence show that MAPK (mitogen-activated protein kinase) plays pleiotrophic role in cell proliferation, differentiation and apoptosis [32]. We further analyzed the effect of emodin on MAPK members in A549 cells. Emodin specifically reduced the levels of phosphorylated ERK, whereas the levels of phosphorylated p38 and JNK did not change (data not shown). To further examine the effect of phosphorylation status of AKT or ERK on emodin-induced apoptosis, inhibitors of PI_3K (LY294002 and Wortamain), ERK inhibitor (U0126 and PD98059) or activator (aurintricarboxylic acid; ATA) were used. As indicated in Fig. 5B, cells grown in the presence of LY294002 or Wortamain, or U0126 were more sensitive to emodin-induced apoptosis. In contrast, the ERK pathway specific activator aurintricarboxylic acid (ATA) significantly blocked the emodin-triggered apoptosis in A549 cells (Fig. 5C).

3.6. Antioxidants block emodin-mediated ROS generation, mitochondrial dysfunction, ERK and AKT inactivation, Bcl-2 increase, Bax decrease, and apoptosis in A549 cells

Finally, an attempt was made to address the hierarchy that might exist between emodin-mediated ROS generation and emodin-induced mitochondrial dysfunction, and perturbations in pro- and anti-apoptotic signaling cascades. A549 cells were treated with emodin in the presence or

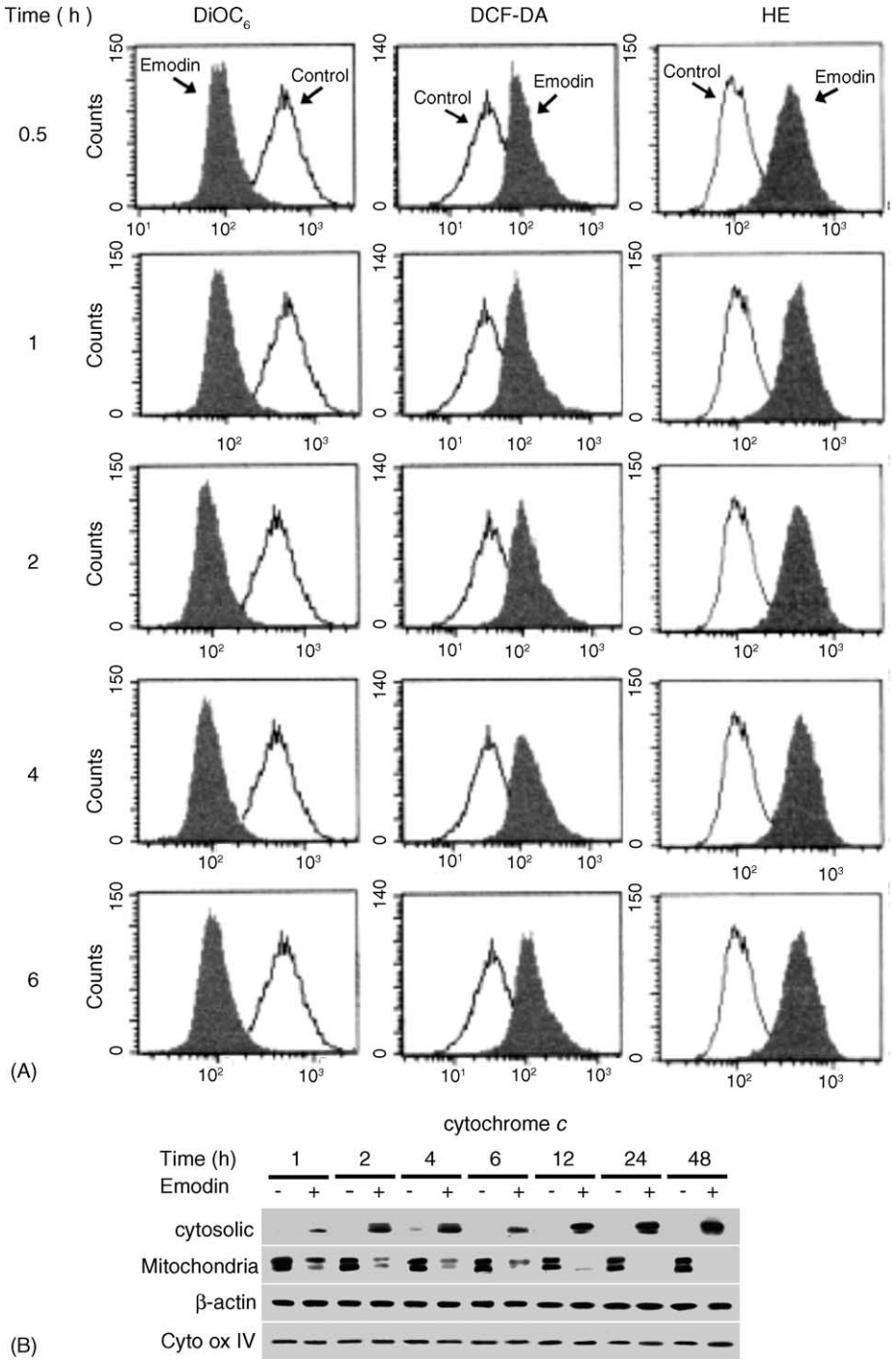

Fig. 3. ROS generation, $\Delta\psi_m$ alteration, and cytochrome *c* release. (A) A549 cells were treated without or with 50 μM emodin for 0.5, 1, 2, 4, and 6 h. Thirty minutes prior to harvesting, cells were incubated with 10 μM HE, 5 μM DCF-DA, or 40 nM $DiOC_6$. After incubation, cell were harvested, and change in fluorescence was measured. (B) Mitochondrial cytochrome *c* release. A549 cells were treated with 50 μM emodin for indicated time points. Cytosolic fraction was isolated, the content of cytochrome *c* was examined by Western blot analysis using anti-cytochrome *c* antibody.

absence of ascorbic acid or NAC. As shown in Fig. 6 with ascorbic acid or *N*-acetylcysteine essentially abrogated emodin-mediated generation of ROS, disruption of mitochondrial membrane potential (Fig. 6A), and apoptosis (Fig. 6B). The protective effects of NAC were not quite as great as those of ascorbic acid. Interestingly, ascorbic acid also blocked emodin-mediated ERK and AKT inactivation, Bcl-2 reduction and Bax elevation (Fig. 6C). Our findings suggest that these events represent downstream consequences of oxidative stress induced by emodin.

4. Discussion

The poor prognostic outcome of lung cancer is due to its resistance to current therapies, maintaining as the leading

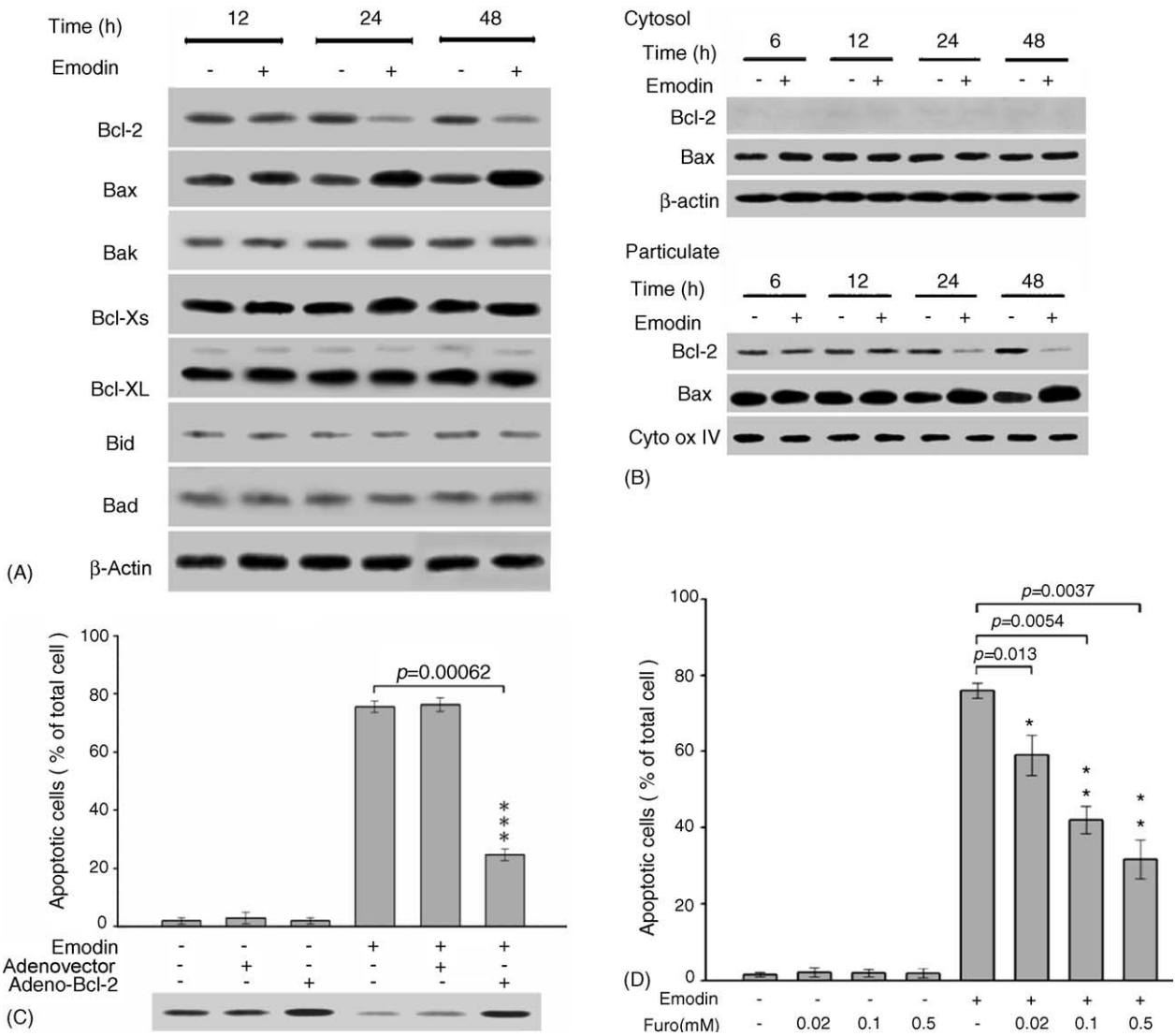

Fig. 4. Involvement of Bcl-2 family proteins in emodin-induced apoptosis. (A) A549 cells were treated with 50 μM emodin for 12, 24, and 48 h. After treatment, cell lysates were extracted, and the levels of Bcl-2 family proteins were analyzed by Western blot analysis. (B) Subcellular distribution of Bcl-2 and Bax proteins. A549 cells were treated with 50 μM emodin for 6, 12, 24 and 48 h. After treatment, cytosolic and particulate fraction were isolated, and analyzed by Western blot for Bcl-2, and Bax. (C) Bcl-2 overexpression inhibited emodin-induced apoptosis. Cells were infected with or without adenovector or adeno-Bcl-2 vector for 4 h, then cells were treated with 50 μM emodin, the levels of Bcl-2 were measured and the apoptotic cells were estimated. (D) Furosemide attenuated emodin-induced apoptosis. A549 cells were treated without or with 50 μM emodin in the absence or presence of 0.02, 0.1, and 0.5 mM furosemide (Furo) for 48 h. After treatment, number of apoptotic cells were determined. Data are presented as mean ± S.D. of nine replicates from three independent experiments.

cause of cancer related death. Successful treatment with chemotherapeutic agents is largely dependent on their ability to trigger cell death in tumor cells; therefore, novel inducers of apoptosis provide a new therapeutic approach for anti-cancer design. Several previous studies demonstrate that certain phytochemicals present in medicinal herbs exerts anti-tumorigenic activity by inducing apoptosis in cancer cells. Emodin has been reported to possess anti-cancer effect on several human cancers in vitro [3,11,12,14–16] and inhibition of malignant transformation and metastasis-associated properties of HER-2/neu overexpression in breast cancer cells in vivo [19]. Emodin also enhanced sensitivity to chemotherapeutic agents in non-small cell lung cancer or breast cancer cells overexpressing HER-2/neu [13,33]. Conversely, it has been reported that emodin enhanced the proliferation of MCF-7 cells [34], and studies demonstrated that emodin had no cytotoxic effect on MCF-7, Hepa-1, HM02, and HepG2 cell lines [5,35]. This report describes the selective in vitro killing of human lung adenocarcinoma A549 cells by emodin, the anti-cancer activity of which is based on apoptotic cell death. The morphology changes of emodin-treated cells were typical of apoptosis, nuclear condensation, DNA fragmentation and caspase activation, all hallmarks of apoptosis. Similar observations have been reported in emodin-treated human cervical cancer cells

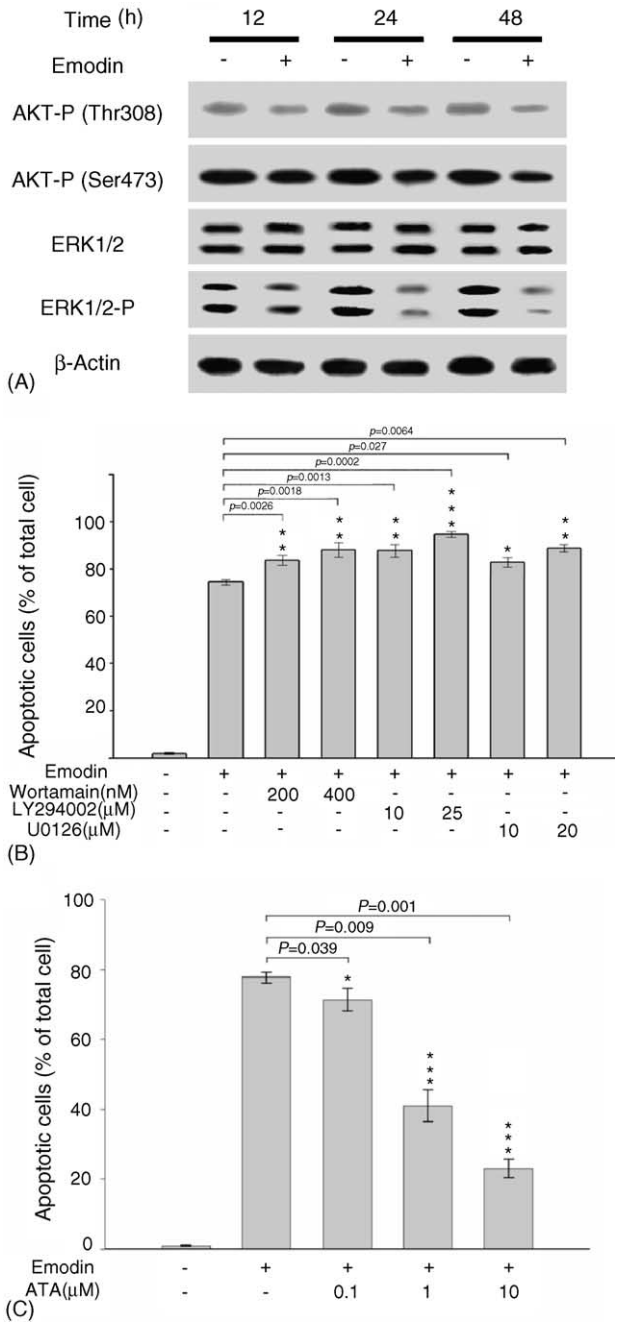

Fig. 5. Inactivation of AKT and ERK were linked to emodin-induced apoptosis. (A) A549 cells were treated without or with 50 μM emodin for 12, 24, and 48 h. After treatment, phosphorylated AKT and ERK were assayed by Western blot analysis. β-Actin was used as an internal control. (B) A549 cells were treated without or with emodin following pretreatment of LY294002, Wortamain, U0126 and (C) ATA for 4 h. After 48 h incubation, apoptotic cells were determined by TUNEL assay. Data are presented as mean ± S.D. of nine replicates from three independent experiments.

[11], human promyeloleukemic HL-60 cells [12], human hepatocarcinoma cell lines [3], and human lung squamous carcinoma cells [15,16]. In addition, our data showed that non-tumor cells such as human fibroblast-like lung WI-38 cells, rat heart endothelial cells, rat hepatic stellate cells, and rat hepatocytes were more resistant to emodin-induced cytotoxic effect, approximately 5, 8, 6, and 10% growth inhibition but not cell death was observed, respectively.

Accumulating evidence indicates that mitochondria play a pivotal role in the apoptotic process in mammalian cells. Disruption of mitochondrial membrane potential ($\Delta\psi_m$) is considered to be an indicator of mitochondria damage and generally is defined as an early stage of apoptosis, preceding efflux of small molecules from the mitochondria (including cytochrome *c*, apoptosis-inducing factor, cIAPs, etc.) and followed by caspase-9/caspase-3 cascade activation [36]. Previous reports indicate that the emodin-induced apoptosis is through a mitochondria-dependent activation of caspase-3 and -9 in human cervical Bu 25 TK cancer cells [11], in human lung squamous carcinoma CH 27 cells [16], and in cultured rat C611B cholangiocarcinoma cells [37]. In the present study, we found that the marked activation of caspases (caspase-2, -3, and -9) by emodin depended on mitochondrial cytochrome *c* release to cytosol, and that it follows the breakdown of $\Delta\psi_m$, suggesting that mitochondria-mediated pathway is involved in emodin-triggered apoptosis. This observation is consistent with the conclusion of a recent study about the effect of emodin in human hepatocarcinoma cell lines [3]. In accordance with our results, Lee et al. reported that aloe-emodin-induced apoptosis was accompanied by Bax upregulation and caspases (caspase-3, -8, and -9) activation in human squamous lung cancer CH27 cells [38]. In our study, treatment of A549 cells with the inhibitor of caspase-9 or caspase-3 drastically blocked apoptosis induced by emodin (Fig. 2C). These results suggest that the intrinsic mitochondria-mediated caspase activation signaling pathway plays a crucial role in emodin-triggered apoptosis.

Furthermore, our results indicated that emodin-induced cytochrome *c* release from mitochondria to cytosol is biphasic. The initial release was preceded by produced oxidative stress caused loss of $\Delta\psi_m$, but the amount of cytochrome *c* release did not commit the cells to the apoptotic pathway. On the other hand, the second phase of cytochrome *c* release, which was of a much greater magnitude and committed the cells to apoptosis, occurred after Bcl-2 and Bax subcellular translocation. Similarly, other author had reported that a biphasic pattern of cytochrome *c* release was seen in human breast cancer MDA-MB 468 cells after exposure to NO [39]. Their results indicate that the second and critical phase of cytochrome *c* release was caused by the overexpression and integration of Bax into mitochondrial membrane and this event was responsible for the commitment of the cells to apoptosis.

Generation of ROS may contribute to mitochondrial damage and lead to cell death by acting as an apoptotic signaling molecules [26]. Several previous studies indicate that emodin (1,3,8-trihydroxy-6-methylanthraquinone) is an anthraquinone with structure similar to that of DMNQ (2,3-dimethoxy-1,4-naphthoquinone) and mitochondrial ubiquinone (Fig. 7), exhibited as a ROS generator to increase the susceptibility of tumor cells to cytotoxic

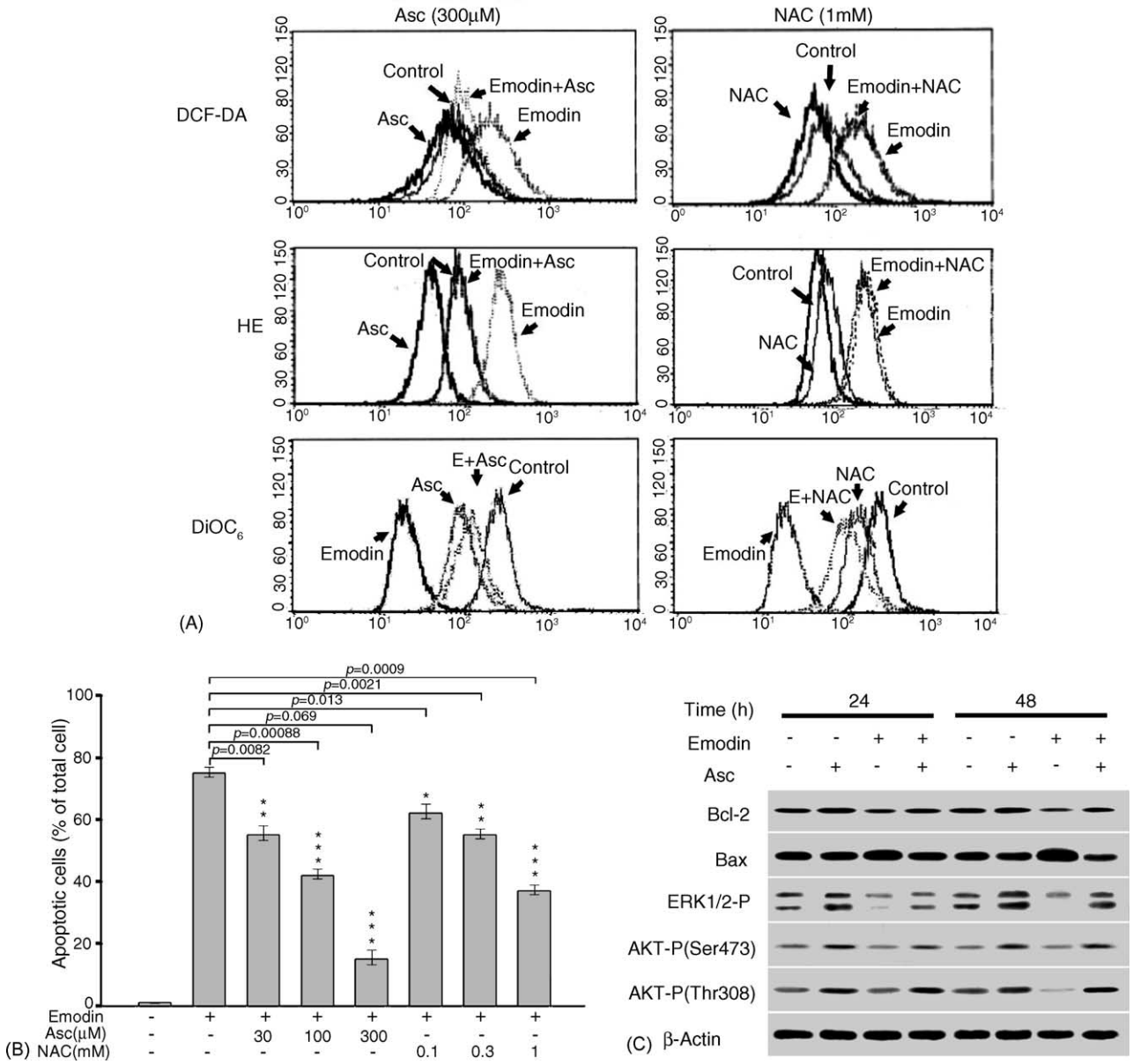

Fig. 6. Antioxidants prevented emodin-triggered ROS generation, $\Delta\psi_m$ disruption, ERK and AKT inactivation, Bcl-2 elevation, Bax reduction, and apoptosis. (A) The effect on ROS and $\Delta\psi_m$. A549 cells were pretreated with 1 mM *N*-acetylcysteine (NAC) or 300 μM of ascorbic acid (Asc) for 30 min, then treated with or without 50 μM emodin for another 1 h. Thirty minute prior to harvesting, cells were incubated with 10 μM HE, 5 μM DCF-DA, and 40 nM $DiOC_6$. After incubation, cell were harvested, the change in fluorescence intensity was measured by flow cytometry. (B) Prevention of apoptosis. Cells were pretreated with various concentrations of NAC or ascorbic acid for 2 h, then treated without or with 50 μM of emodin for another 48 h. After treatment, apoptotic cells were measured using TUNEL assay by flow cytometry. Data are presented as mean ± S.D. of nine replicates from three independent experiments. (C) Ascorbic acid (Asc) reversed emodin-mediated anti- or pro-apoptotic signaling molecules. A549 cells were pretreatment of 300 μM ascorbic acid for 2 h, then incubated without or with 50 μM emodin for 24 and 48 h. After treatment, cell lysates were extracted, the level of Bax, Bcl-2, phosphorylated AKT (AKT-P), and phosphorylated ERK (ERK-P) were analyzed by Western blot analysis.

therapeutic agents [18,40–42]. Quinones are highly redox active molecules, which can redox cycle with their semiquinone radicals, leading to the formation of reactive oxygen species that include the superoxide anion radical, the peroxyl radical, hydrogen peroxide and, ultimately, the hydroxyl radical [43–45]. A previous study had been demonstrated that the quinoid structure of emodin could be activated to the semiquinone radical intermediate, which in turn could react with oxygen to produce superoxide anion radical, hydrogen peroxide, and hydroxyl radical [46]. Several studies indicate that emodin-induced apoptosis is mediated by ROS generated from the semiquinone [8,46]. Here, we found that in addition to its effect on mitochondrial membrane potential ($\Delta\psi_m$), emodin caused an increase in ROS production in A549 cells. The emodin-mediated disruption of $\Delta\psi_m$ and apoptosis in A549 cells is apparently dependent on ROS generation because the emodin-mediated $\Delta\psi_m$ disruption and apop-

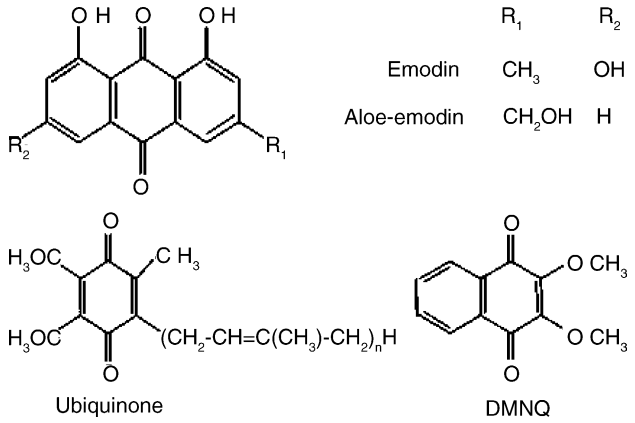

Fig. 7. The chemical structures of emodin-related compounds.

tosis can be abolished or attenuated by the antioxidants, ascorbic acid and *N*-acetylcysteine. However, the results from Chen et al. demonstrate that emodin-induced apoptosis in human promyeloleukemic HL-60 cells is ROS independent [12]. The discrepancies in Chen et al. and ours may be due to different cell lines used. The present study showed that an early and rapid generation of ROS by emodin plays a central role in apoptotic process. Similarly, a previous report demonstrated that MS-275 (a histone deacetylase inhibitor)-induced ROS generation occurred at very early intervals (~2 h) and clearly preceded other hallmarks of apoptosis, such as release of mitochondrial cytochrome *c* and activation of caspases (minimal changes were observed at 24 h, peaked at 48 h) [47]. Moreover, treatment of human melanoma SK-MEL-2 cells with asiatic acid caused a ROS-mediated apoptosis. The asiatic acid-induced generation of ROS was observed as early as at 15 min, while upregulation of Bax was detected at 12 h, and caspase-3 remained activated 48 h after addition of asiatic acid [48]. These observations suggest that early and rapid ROS generation can act as an important determinant of apoptotic cell death induced by many different stimuli.

Bcl-2 is localized in the mitochondria, endoplasmic reticulum, and nuclear membranes, where most of the oxygen-free radicals are generated and where the free radicals exert their apoptotic effects. Bcl-2 probably acts to prevent apoptosis by scavenging oxygen derived free radicals inside the cells [49]. Treatment of A549 cells with emodin decreased the Bcl-2 and increased the Bax protein levels. The increase in the content of Bax was followed by the translocation of this protein to the mitochondria. The pro-apoptotic action of Bax is known to be mediated by its insertion into the outer mitochondrial membrane. Upon its translocation to the mitochondria, Bax can cause the release of cytochrome *c* and induce cell death. Treatment with the chloride inhibitor furosemide reduced the translocation of Bax to the mitochondria, consequently, furosemide prevented the release of cytochrome *c* from the mitochondrial and reduced the extent of cell killing [30]. Moreover, our data demonstrated that antioxidant ascorbic acid reversed the emodin-mediated Bcl-2 and Bax cellular content and reduced the loss of viability. Similarly, ascorbic acid and α-tocopherol have been shown to prevent lipopolysaccharide-induced apoptosis by modulation of Bcl-2 and Bax proteins [50]. These results suggest that ROS might modulate the cellular distribution and content of Bcl-2 and Bax.

It is noteworthy that phosphorylation of AKT, a PI_3-kinase down stream molecules is anti-apoptotic [51]. Inhibition of this kinase by LY294002 or wortmannin potentiates apoptotic cell death [52]. Previous reports indicated that translocation of Bax from the cytosol to the mitochondria can be modulated by the PI3-kinase/AKT pathway [31,53]. A recent report demonstrates that emodin-triggered apoptosis is through a mechanism involving inactivation of AKT [37]. Consistently, our observations showed that exposure of A549 cells to emodin resulted in AKT inactivation. Moreover, treatment with LY294002 or wortmannin acceleration of cell killing by emodin may be reflecting inactivation of AKT involved in emodin-triggered death process. However, whether the translocation of Bax was regulated by AKT in emodin-treated A549 cells remains to be defined. It has been reported that among the three type of mitogen-activated protein kinase, p38 and c-Jun-N-terminal protein kinase (JNK) are predominately activated in response to cellular redox stress, but not extracellular signal-regulated kinase (ERK) [54]. However, the nature of the relationship that may exist between MAPK pathways and oxidative stress has not yet been completely defined in neoplastic cells undergoing apoptosis in response to emodin. The results presented here indicated that emodin-induced ROS generation and apoptosis was associated with ERK inactivation. Moreover, emodin lethality was potentiated by pharmacologic MEK inhibitors (U0126 and PD98059). Conversely, stimulation of ERK activation by ATA attenuated emodin lethality in A549 cells. Consistently with our finding for emodin, Huang [55] has previously presented data demonstrating that inactivation of ERK but not p38 is an important determinant of apoptotic cell death induced by emodin in cultured human breast cancer MDA-MB-231 cells and human skin squamous carcinoma HSC5 cells. At present, it is still not clear how emodin affects MAPK signaling pathways. Since emodin has been shown to display highly selective activity against ras-oncogene [56], it is possible that this suppression leads to inhibition of ERK phosphorylation and activation. While the mechanism by which ERK activation might protect cells from emodin-induced lethal events is uncertain, several possibilities have been proposed, including phosphorylation of Bad or procaspase-9 [57,58]. Whether any of these events are involved in the protective effects of ERK in emodin-treated cells remains to be clarified.

In conclusion, the emodin-induced apoptotic events can be summarized by the sequence presented in Fig. 8. In this model, emodin-mediated ROS generation represents the

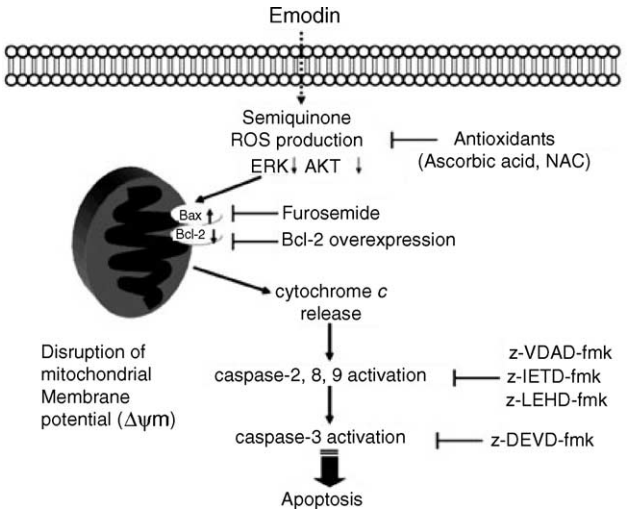

Fig. 8. A model for summarizing emodin-induced apoptosis pathway in human lung adenocarcinoma A549 cells.

central trigger for activation of the apoptotic cascade. Exposure of A549 cells to emodin resulted in generation of ROS and a decrease in $\Delta\psi_m$, downregulation of the cytoprotective ERK and AKT cascade, as well as in elevation of Bax and reduction of Bcl-2 levels, the movement of Bax to the mitochondria reduced the $\Delta\psi_m$, an event that results in the release of cytochrome *c*, subsequently activation of caspase-2, -3, and -9, and consequently cleaved specific substrates leading to apoptotic changes. These findings may aid in the understanding of the mode of actions of the emodin and provide a theoretical basis for the therapeutic use of this compound.

Acknowledgments

This work is supported by grants from the Taichung Veterans General Hospital TCVGH-927312D and National Science Council NSC92-2311-B-075A-001, Taiwan, Republic of China.

References

[1] Chang GC, Chen KC, Yang TY, Yin MC, Lin CP, Kuo BI, et al. Activity of gefitinib in advanced non-small-cell lung cancer with very poor performance status. Invest New Drugs 2005;23:73–7.
[2] Carnero A. Targeting the cell cycle for cancer therapy. Br J Cancer 2002;87:129–33.
[3] Jing X, Ueki N, Cheng J, Imanishi H, Hada T. Induction of apoptosis in hepatocellular carcinoma cell lines by emodin. Jpn J Cancer Res 2002;93:874–82.
[4] Hu W, Kavanagh JJ. Anticancer therapy targeting the apoptotic pathway. Lancet Oncol 2003;4:721–9.
[5] Demirezer LO, Kuruuzum-Uz A, Bergere I, Schiewe HJ, Zeeck A. The structures of antioxidant and cytotoxic agents from natural source: anthraquinones and tannins from roots of Rumex patientia. Phytochemistry 2001;58:1213–7.
[6] Wang HH, Chung JG. Emodin-induced inhibition of growth and DNA damage in the Helicobacter pylori. Curr Microbiol 1997;35:262–6.
[7] Chang CH, Lin CC, Yang JJ, Namba T, Hattori M. Anti-inflammatory effects of emodin from ventilago leiocarpa. Am J Chin Med 1996;24:139–42.
[8] Huang HC, Chang JH, Tung SF, Wu RT, Foegh ML, Chu SH. Immunosuppressive effect of emodin, a free radical generator. Eur J Pharmacol 1992;211:359–64.
[9] Sato M, Maulik G, Bagchi D, Das DK. Myocardial protection by protykin, a novel extract of trans-resveratrol and emodin. Free Radic Res 2000;32:135–44.
[10] Goel RK, Das Gupta G, Ram SN, Pandey VB. Antiulcerogenic and anti-inflammatory effects of emodin, isolated from Rhamnus triquerta wall. Indian J Exp Biol 1991;29:230–2.
[11] Srinivas G, Anto RJ, Srinivas P, Vidhyalakshmi S, Senan VP, Karunagaran D. Emodin induces apoptosis of human cervical cancer cells through poly(ADP-ribose) polymerase cleavage and activation of caspase-9. Eur J Pharmacol 2003;473:117–25.
[12] Chen YC, Shen SC, Lee WR, Hsu FL, Lin HY, Ko CH, et al. Emodin induces apoptosis in human promyeloleukemic HL-60 cells accompanied by activation of caspase 3 cascade but independent of reactive oxygen species production. Biochem Pharmacol 2002;64:1713–24.
[13] Zhang L, Lau YK, Xi L, Hong RL, Kim DS, Chen CF, et al. Tyrosine kinase inhibitors, emodin and its derivative repress HER-2/neu-induced cellular transformation and metastasis-associated properties. Oncogene 1998;16:2855–63.
[14] Zhang L, Chang CJ, Bacus SS, Hung MC. Suppressed transformation and induced differentiation of HER-2/neu-overexpressing breast cancer cells by emodin. Cancer Res 1995;55:3890–6.
[15] Lee HZ. Protein kinase C involvement in aloe-emodin- and emodin-induced apoptosis in lung carcinoma cell. Br J Pharmacol 2001;134:1093–103.
[16] Lee HZ. Effects and mechanisms of emodin on cell death in human lung squamous cell carcinoma. Br J Pharmacol 2001;134:11–20.
[17] Jayasuriya H, Koonchanok NM, Geahlen RL, McLaughlin JL, Chang CJ. Emodin, a protein tyrosine kinase inhibitor from Polygonum cuspidatum. J Nat Prod 1992;55:696–8.
[18] Yi J, Yang J, He R, Gao F, Sang H, Tang X, et al. Emodin enhances arsenic trioxide-induced apoptosis via generation of reactive oxygen species and inhibition of survival signaling. Cancer Res 2004;64:108–16.
[19] Zhang L, Lau YK, Xia W, Hortobagyi GN, Hung MC. Tyrosine kinase inhibitor emodin suppresses growth of HER-2/neu-overexpressing breast cancer cells in athymic mice and sensitizes these cells to the inhibitory effect of paclitaxel. Clin Cancer Res 1999;5:343–53.
[20] Richards PS, Saba TM, Del Vecchio PJ, Vincent PA, Gray VC. Matrix fibronectin disruption in association with altered endothelial cell adhesion induced by activated polymorphonuclear leukocytes. Exp Mol Pathol 1986;45:1–21.
[21] Kang YH, Berthiaume F, Nath BD, Yarmush ML. Growth factors and nonparenchymal cell conditioned media induce mitogenic responses in stable long-term adult rat hepatocyte cultures. Exp Cell Res 2004;293:239–47.
[22] Chen Z, Zhang X, Li M, Wang Z, Wieand HS, Grandis JR, et al. Simultaneously targeting epidermal growth factor receptor tyrosine kinase and cyclooxygenase-2, an efficient approach to inhibition of squamous cell carcinoma of the head and neck. Clin Cancer Res 2004;10:5930–9.
[23] Yang SE, Hsieh MT, Tsai TH, Hsu SL. Down-modulation of Bcl-XL, release of cytochrome *c* and sequential activation of caspases during honokiol-induced apoptosis in human squamous lung cancer CH27 cells. Biochem Pharmacol 2002;63:1641–51.
[24] Rosse T, Olivier R, Monney L, Rager M, Conus S, Fellay I, et al. Bcl-2 prolongs cell survival after Bax-induced release of cytochrome *c*. Nature 1998;391:496–9.
[25] Vaux DL, Korsmeyer SJ. Cell death in development. Cell 1999; 96:245–54.

[26] Martindale JL, Holbrook NJ. Cellular response to oxidative stress: signaling for suicide and survival. J Cell Physiol 2002;192:1–15.
[27] Simon HU, Haj-Yehia A, Levi-Schaffer F. Role of reactive oxygen species (ROS) in apoptosis induction. Apoptosis 2000;5:415–8.
[28] Antonsson B. Bax and other pro-apoptotic Bcl-2 family "killer-proteins" and their victim the mitochondrion. Cell Tissue Res 2001;306:347–61.
[29] Krajewski S, Tanaka S, Takayama S, Schibler MJ, Fenton W, Reed JC. Investigation of the subcellular distribution of the bcl-2 oncoprotein: residence in the nuclear envelope, endoplasmic reticulum, and outer mitochondrial membranes. Cancer Res 1993;53:4701–14.
[30] Tafani M, Cohn JA, Karpinich NO, Rothman RJ, Russo MA, Farber JL. Regulation of intracellular pH mediates Bax activation in HeLa cells treated with staurosporine or tumor necrosis factor-alpha. J Biol Chem 2002;277:49569–76.
[31] Yamaguchi H, Wang HG. The protein kinase PKB/Akt regulates cell survival and apoptosis by inhibiting Bax conformational change. Oncogene 2001;20:7779–86.
[32] Tournier C, Hess P, Yang DD, Xu J, Turner TK, Nimnual A, et al. Requirement of JNK for stress-induced activation of the cytochrome *c*-mediated death pathway. Science 2000;288:870–4.
[33] Zhang L, Hung MC. Sensitization of HER-2/neu-overexpressing non-small cell lung cancer cells to chemotherapeutic drugs by tyrosine kinase inhibitor emodin. Oncogene 1996;12:571–6.
[34] Matsuda H, Shimoda H, Morikawa T, Yoshikawa M. Phytoestrogens from the roots of Polygonum cuspidatum (Polygonaceae): structure-requirement of hydroxyanthraquinones for estrogenic activity. Bioorg Med Chem Lett 2001;11:1839–42.
[35] Zhang S, Qin C, Safe SH. Flavonoids as aryl hydrocarbon receptor agonists/antagonists: effects of structure and cell context. Environ Health Perspect 2003;111:1877–82.
[36] Green DR, Reed JC. Mitochondria and apoptosis. Science 1998;281: 1309–12.
[37] Lai GH, Zhang Z, Sirica AE. Celecoxib acts in a cyclooxygenase-2-independent manner and in synergy with emodin to suppress rat cholangiocarcinoma growth in vitro through a mechanism involving enhanced Akt inactivation and increased activation of caspases-9 and -3. Mol Cancer Ther 2003;2:265–71.
[38] Lee HZ, Hsu SL, Liu MC, Wu CH. Effects and mechanisms of aloe-emodin on cell death in human lung squamous cell carcinoma. Eur J Pharmacol 2001;431:287–95.
[39] Pervin S, Singh R, Chaudhuri G. Nitric-oxide-induced Bax integration into the mitochondrial membrane commits MDA-MB-468 cells to apoptosis: essential role of Akt. Cancer Res 2003;63:5470–9.
[40] Gao F, Yi J, Shi GY, Li H, Shi XG, Tang XM. The sensitivity of digestive tract tumor cells to As_2O_3 is associated with the inherent cellular level of reactive oxygen species. World J Gastroenterol 2002; 8:36–9.
[41] Yi J, Gao F, Shi G, Li H, Wang Z, Shi X, et al. The inherent cellular level of reactive oxygen species: one of the mechanisms determining apoptotic susceptibility of leukemic cells to arsenic trioxide. Apoptosis 2002;7:209–15.
[42] Yang J, Li H, Chen YY, Wang XJ, Shi GY, Hu QS, et al. Anthraquinones sensitize tumor cells to arsenic cytotoxicity in vitro and in vivo via reactive oxygen species-mediated dual regulation of apoptosis. Free Radic Biol Med 2004;37:2027–41.
[43] Watanabe N, Forman HJ. Autoxidation of extracellular hydroquinones is a causative event for the cytotoxicity of menadione and DMNQ in A549-S cells. Arch Biochem Biophys 2003;411: 145–57.
[44] Goulart MO, Falkowski P, Ossowski T, Liwo A. Electrochemical study of oxygen interaction with lapachol and its radical anions. Bioelectrochemistry 2003;59:85–7.
[45] Sugawara M, Sugawara Y, Wen K, Giulivi C. Generation of oxygen free radicals in thyroid cells and inhibition of thyroid peroxidase. Exp Biol Med (Maywood) 2002;227:141–6.
[46] Pry or WA. Free radical biology: xenobiotics, cancer, and aging. Ann N Y Acad Sci 1982;393:1–22.
[47] Rosato RR, Almenara JA, Grant S. The histone deacetylase inhibitor MS-275 promotes differentiation or apoptosis in human leukemia cells through a process regulated by generation of reactive oxygen species and induction of p21CIP1/WAF1 1. Cancer Res 2003;63: 3637–45.
[48] Park BC, Bosire KO, Lee ES, Lee YS, Kim JA. Asiatic acid induces apoptosis in SK-MEL-2 human melanoma cells. Cancer Lett 2005;218:81–90.
[49] Hockenbery DM, Oltvai ZN, Yin XM, Milliman CL, Korsmeyer SJ. Bcl-2 functions in an antioxidant pathway to prevent apoptosis. Cell 1993;75:241–51.
[50] Haendeler J, Zeiher AM, Dimmeler S. Vitamin C and E prevent lipopolysaccharide-induced apoptosis in human endothelial cells by modulation of Bcl-2 and Bax. Eur J Pharmacol 1996;317: 407–11.
[51] Datta SR, Dudek H, Tao X, Masters S, Fu H, Gotoh Y, et al. Akt phosphorylation of BAD couples survival signals to the cell-intrinsic death machinery. Cell 1997;91:231–41.
[52] Xu J, Liao K. Protein kinase B/AKT 1 plays a pivotal role in insulin-like growth factor-1 receptor signaling induced 3T3-L1 adipocyte differentiation. J Biol Chem 2004;279:35914–22.
[53] Tsuruta F, Masuyama N, Gotoh Y. The phosphatidylinositol 3-kinase (PI3K)-Akt pathway suppresses Bax translocation to mitochondria. J Biol Chem 2002;277:14040–7.
[54] Kyriakis JM, Avruch J. Mammalian mitogen-activated protein kinase signal transduction pathways activated by stress and inflammation. Physiol Rev 2001;81:807–69.
[55] Huang Q, Shen HM, Ong CN. Inhibitory effect of emodin on tumor invasion through suppression of activator protein-1 and nuclear factor-kappaB. Biochem Pharmacol 2004;68:361–71.
[56] Chang CJ, Ashendel CL, Geahlen RL, McLaughlin JL, Waters DJ. Oncogene signal transduction inhibitors from medicinal plants. In Vivo 1996;10:185–90.
[57] Allan LA, Morrice N, Brady S, Magee G, Pathak S, Clarke PR. Inhibition of caspase-9 through phosphorylation at Thr 125 by ERK MAPK. Nat Cell Biol 2003;5:647–54.
[58] Scheid MP, Schubert KM, Duronio V. Regulation of bad phosphorylation and association with Bcl-x(L) by the MAPK/Erk kinase. J Biol Chem 1999;274:31108–13.